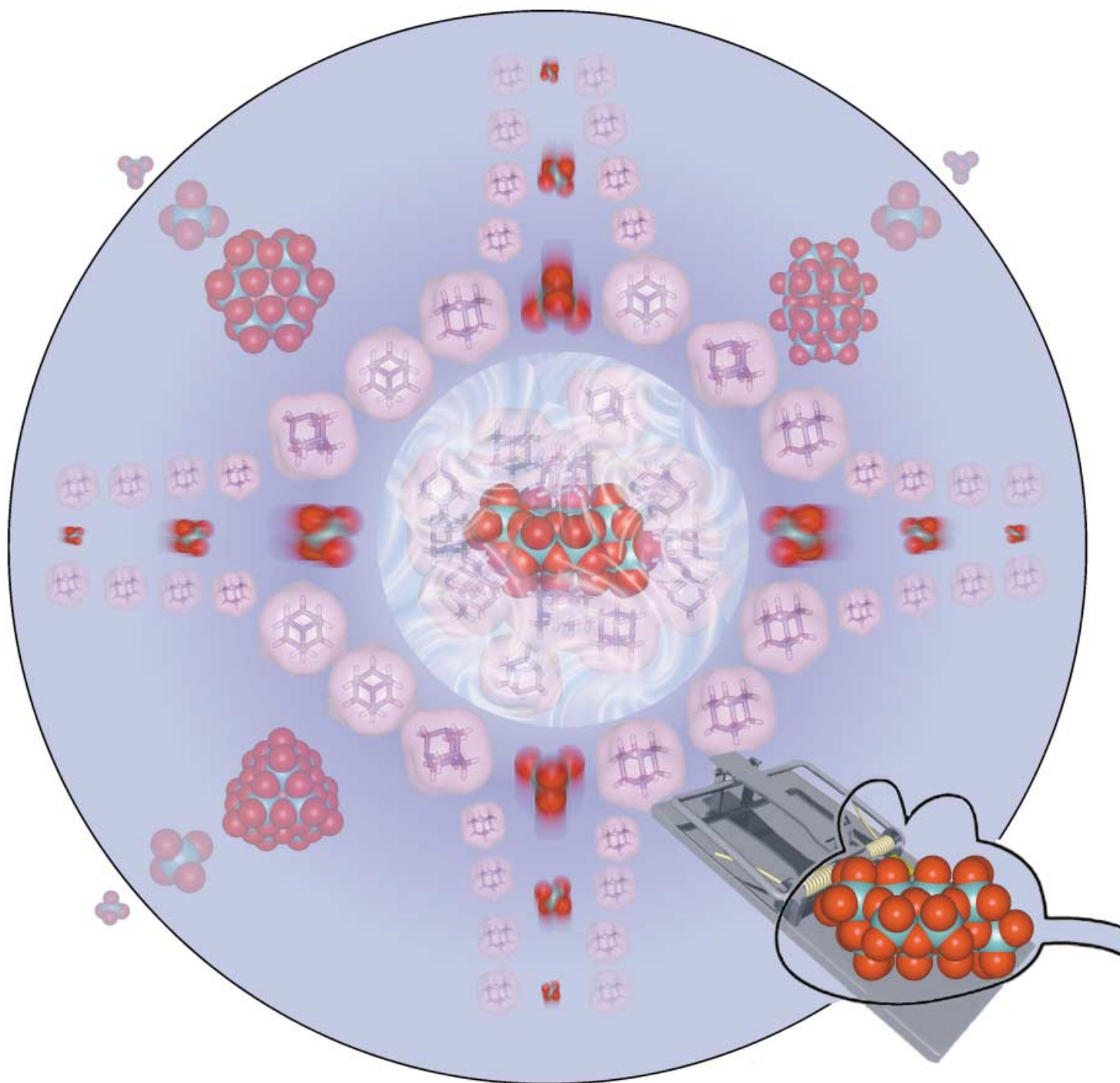


# Zuschriften



Durch „Einschweißen“ mit großen organischen Kationen können instabile unsymmetrische Polyoxometallate abgefangen und isoliert werden. Die Methode verhindert die Umlagerung und Aggregation der Clustereinheiten zu höher symmetrischen Strukturen. Erste Reaktivitätsstudien mit solchen „eingeschweißten“ Clustern präsentieren L. Cronin et al. auf den folgenden Seiten.

# Restraining Symmetry in the Formation of Small Polyoxomolybdates: Building Blocks of Unprecedented Topology Resulting From “Shrink-Wrapping” $[\text{H}_2\text{Mo}_{16}\text{O}_{52}]^{10-}$ -Type Clusters\*\*

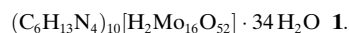
De-Liang Long, Paul Kögerler, Louis J. Farrugia, and Leroy Cronin\*

Dedicated to Professor Achim Müller on the occasion of his 65th Birthday

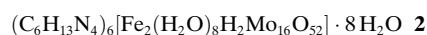
The structural diversity and potential for the formation of nanoscopic molecules in the field of polyoxomolybdate (POMo) cluster chemistry has been recently demonstrated in dramatic fashion.<sup>[1]</sup> Sparked by these discoveries and the many applications found and proposed for POMo-based clusters,<sup>[2–4]</sup> interest in their rational synthesis has been increasing rapidly. For example, the concept of generating a set of linkable nucleophilic building blocks that can be condensed together according to their intrinsic geometric and electronic properties has been stimulating research on the design of POMos with both high<sup>[5]</sup> and low<sup>[6]</sup> nuclearities. A range of smaller polyanions have themselves been incorporated as building blocks into hybrid and network solids,<sup>[7]</sup> however, there has been little advance in the generation of fundamentally new types of pure Mo–O cluster frameworks in the small-to-medium nuclearity range ( $\text{Mo}_{10}$ – $\text{Mo}_{18}$ ). Therefore, to expand this building-block concept further, the construction of structurally diverse cluster and cluster-based network geometries calls for the generation and isolation of low-nuclearity polyoxometalates that substantially deviate from the well-known “classical” polyoxometalate prototypes. These prototypes include clusters with spherical structures and high symmetry, such as the Lindqvist, Keggin, or Dawson anions.<sup>[8]</sup> Access to new types of nonspherical, low-symmetry clusters that can be used as building blocks (i.e., that display high negative charge and nucleophilicity) will be significant as their low symmetries are a crucial prerequisite for the emergence of structural complexity when tiling or linking these building blocks to larger aggregates.<sup>[9]</sup> To accomplish

this, we have adopted a simple strategy to prevent the rapid aggregation of metal-oxide-based polyhedra to clusters with a stable uniform spherical topology. This approach relies on trapping and stabilizing nonspherical polyanions of low nuclearity and symmetry before their aggregation and rearrangement to more uniform and stable structures.

By adopting this approach we have synthesized a mixed-valence cluster anion which results when the formation of symmetrical aggregates appears to be restrained by “shrink-wrapping” the anionic POMo cluster. As such the cluster comprises a type of polyoxometalate cluster framework that displays an unprecedented topology, low symmetry, and high negative charge, and is isolated as:



The anion in compound **1** demonstrates a high nucleophilicity and can bind two divalent transition-metal ions ( $\text{Fe}^{\text{II}}$ ,  $\text{Mn}^{\text{II}}$ ,  $\text{Co}^{\text{II}}$ ,  $\text{Ni}^{\text{II}}$ , or  $\text{Zn}^{\text{II}}$ ) to its framework. This yields a family of isostructural complexes, as confirmed by powder diffraction studies, and we have been able to determine the structure of an iron-adduct cluster **2**, which shows that the basic topology found for the anion in compound **1** is maintained. Hence, **2** can be formulated as:



By using protonated hexamethylenetetraamine ( $\text{HMTAH}^+$  or  $\text{C}_6\text{H}_{13}\text{N}_4^+$ ) as counterions, the cluster compounds **1** and **2** were isolated as crystalline precipitates from an acidified molybdate solution in the presence of a reducing agent in around 20–30 % yield.<sup>[10]</sup> Compounds **1** and **2** were characterized by single-crystal X-ray structure analyses,<sup>[11]</sup> bond valence sum (BVS) calculations, redox titrations, and elemental analyses, to aid in the determination of the (formal) number of  $\text{Mo}^{\text{V}}$  centers and protonation sites,<sup>[12]</sup> and also using IR and UV/Vis spectroscopy, and magnetic susceptibility measurements. In addition, the purity of the bulk phase of compounds **1** and **2** has also been confirmed by X-ray powder diffraction.

X-ray crystallographic analysis of **1** reveals that the anions present consist of a highly negatively charged framework of the composition  $[\text{H}_2\text{Mo}_{16}\text{O}_{52}]^{10-}$  (Figure 1). The cluster framework displays an unusual flat shape and despite its high charge and nonspherical structure, this mixed-valence cluster compound is stable in the solid state as the salt **1**. Redox titrations, bond valence sum calculations, and elemental analysis reveal the formal oxidation numbers of the Mo centers to be  $\text{Mo}_4^{\text{V}}\text{Mo}_{12}^{\text{VI}}$ . The four  $\text{Mo}^{\text{V}}$  centers comprise two centrosymmetrically related  $\text{Mo}_2^{\text{V}}$  groups (located in the central part of the  $[\text{H}_2\text{Mo}_4^{\text{V}}\text{Mo}_{12}^{\text{VI}}\text{O}_{52}]^{10-}$  cluster core) which display a short Mo(2)–Mo(3) contact of 2.6427(4) Å, which is characteristic of Mo–Mo single bonds, and also explains the brown color<sup>[12]</sup> that is associated with clusters containing these groups.<sup>[13]</sup> The shape of the cluster resembles that of a “bat” and its main “body” consists of a central unit with twelve molybdenum atoms and two “wings” each with two molybdenum centers (according to the formulation  $[\{\text{Mo}_{12}\} + 2\{\text{Mo}_2\}]$ ). In contrast to known polyoxomolybdates, **1** has a

[\*] Dr. L. Cronin, Dr. D.-L. Long, Dr. L. J. Farrugia  
Department of Chemistry  
Joseph Black Building, The University of Glasgow  
University Avenue, Glasgow, G12 8QQ (UK)  
Fax: (+44) 141 330 4888  
E-mail: L.Cronin@chem.gla.ac.uk

Dr. P. Kögerler  
Ames Laboratory and Department of Physics & Astronomy  
Iowa State University  
Ames, IA 50011 (USA)

[\*\*] This work was supported by the Leverhulme Trust (London), The Royal Society, and The University of Glasgow. The EPSRC provided funds for the X-ray diffractometer. We would like to acknowledge Dr. B. M. Kariuki (University of Birmingham (UK)) for help with initial crystallographic studies.

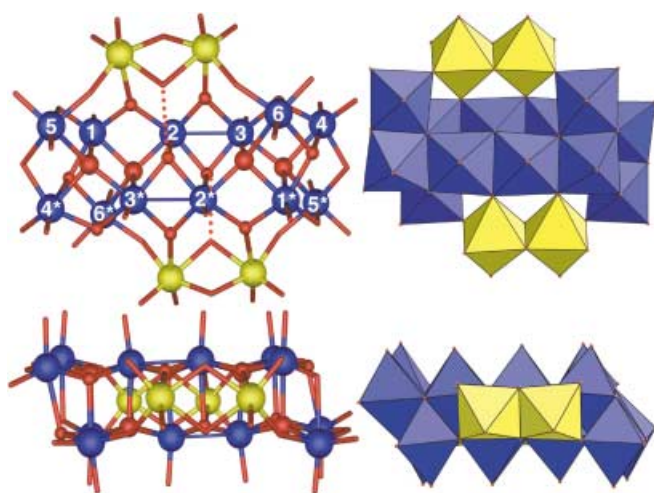


**Figure 1.** Ball-and-stick (left) and polyhedral representations (right) of the crystal structure of the  $[\text{H}_2\text{Mo}^{\text{V}}_4\text{Mo}^{\text{VI}}_{12}\text{O}_{52}]^{10-}$  anion in **1** (top views above and side views below). The Mo positions 1 to 4 and 1\* to 4\* form the two  $\{\text{Mo}_4\}$  backbones, in which 2, 2\*, 3, and 3\* are the reduced  $\text{Mo}^{\text{V}}$  centers (centrosymmetrically equivalent positions are indicated by a star). The Mo positions 5, 5\*, 6, and 6\* cap the ends of the backbones. The  $\mu_4$ -oxo groups are shown by the large red spheres, the  $\mu_3$ -oxo groups by smaller red spheres, and the  $\mu_2$ -oxo bridging and terminal oxo ligands as red sticks. Finally, the two  $\{\text{Mo}_2\}$  “wings” are shown in yellow and the hydrogen bonds are indicated by red dotted lines. The bond lengths for all terminal  $\text{Mo}=\text{O}$  bonds range from 1.687(3) to 1.730(3) Å, while the bridging  $\text{O}-\text{Mo}$  bonds range from 1.752(2) to 2.394(2) Å.

flat structure with approximate dimensions of  $13 \times 11 \times 6$  Å. Of the twelve molybdenum centers which form the main body of the “bat”, eight molybdenum centers are arranged in two lines of four to form two  $\{\text{Mo}_4\}$  “backbones”, which are highly condensed. This is illustrated by the large number of bridging oxo ligands in this central fragment, which comprises 18 (four  $\mu_4$ -oxo, ten  $\mu_3$ -oxo, and four  $\mu_2$ -oxo ligands) of the 52 oxo ligands in total. The two protons in the  $[\text{H}_2\text{Mo}^{\text{V}}_4\text{Mo}^{\text{VI}}_{12}\text{O}_{52}]^{10-}$  anion are involved in hydrogen-bonding interactions between the backbone and the wings, highlighted in Figure 1 as red dotted lines ( $\text{O}\cdots\text{O}$ : 2.732(5) Å).<sup>[11]</sup>

Complex **2** can be isolated as the salt  $(\text{C}_6\text{H}_{13}\text{N}_4)_6[\text{Fe}_2(\text{H}_2\text{O})_8\text{H}_2\text{Mo}^{\text{V}}_4\text{Mo}^{\text{VI}}_{12}\text{O}_{52}] \cdot 8\text{H}_2\text{O}$  and consists of  $[\text{Fe}_2(\text{H}_2\text{O})_8\text{H}_2\text{Mo}^{\text{V}}_4\text{Mo}^{\text{VI}}_{12}\text{O}_{52}]^{6-}$  cluster anions,  $\text{HMTAH}^+$  cations, and solvent water molecules. The polyoxomolybdate anion present in **2** (Figure 2) is derived from the cluster  $[\text{H}_2\text{Mo}^{\text{V}}_4\text{Mo}^{\text{VI}}_{12}\text{O}_{52}]^{10-}$  anion in **1** with its structural features retained, and in **2** the two  $[\text{Fe}^{\text{II}}(\text{H}_2\text{O})_4]$  units are each coordinated to two terminal oxo ligands attached to  $\text{Mo}^{\text{VI}}(4)$  and  $\text{Mo}^{\text{V}}(3)$  (as labeled in the parent anion shown in Figure 1) at the opposite ends of the central  $\{\text{Mo}_{12}\}$  body of the polyoxomolybdate anion. The coordination of the  $\text{Fe}^{\text{II}}$  centers to these particular sites is unexpected as semiempirical and preliminary DFT calculations of the cluster anion suggest that, among all terminal neighbored oxygen positions in the cluster anion in **1** that allow both steric access and a bidentate chelating coordination to a  $\text{M}^{2+}$  ion, the particular  $\text{O}(\text{Mo}3)$  and  $\text{O}(\text{Mo}4)$  positions actually display the lowest negative partial charges.<sup>[14]</sup>

While compound **1** is diamagnetic because of strong antiferromagnetic exchange within each of the two pairs of  $\text{Mo}^{\text{V}}_2$  units (with  $\chi_{\text{dia/TIP}} = -1.1 \times 10^{-3} \text{ emu mol}^{-1}$ ; TIP = temperature independent paramagnetism), the magnetic properties of **2** indicate weak, yet significant, intramolecular antiferromagnetic exchange interactions between the two  $\text{Fe}^{\text{II}}$  centers, despite their wide spatial separation of 1.18 nm. The observed temperature dependence of the susceptibility ( $2 \text{ K} < T < 290 \text{ K}$ , 0.5 T, corrected for  $\chi_{\text{dia}} = -9.0 \times 10^{-4} \text{ emu mol}^{-1}$ ) is best fitted to a Heisenberg model, employing the spin Hamiltonian  $\mathcal{H} = -J\hat{S}_1\hat{S}_2 + \hat{S}_1\mathbf{D}\hat{S}_1 + \hat{S}_2\mathbf{D}\hat{S}_2$ , with an exchange constant  $J = -0.8 \text{ K}$  and a single-ion anisotropy  $D = 8 \text{ K}$  (reflecting the zero-field splitting of the  $^5T_2$  term of the high-spin  $3d^6$   $\text{Fe}^{\text{II}}$  centers in an octahedral field). This exemplifies the efficiency of reduced polyoxomolybdates to act as superexchange ligands, where in the present case the superexchange pathways involve at least six centers and both  $\{\text{Mo}_2\}$  dimers of the  $\{\text{Mo}_{16}\}$  framework. The encapsulation of the cluster anion also effectively prevents any significant intercluster exchange interactions. Antiferromagnetic (yet weaker) coupling is also observed for the other magnetic derivatives  $\{\text{Mn}^{\text{II}}_2\text{Mo}_{16}\}$  and  $\{\text{Ni}^{\text{II}}_2\text{Mo}_{16}\}$  in the isostructural series of **2**.

An interesting aspect of the encapsulation is that it appears to also cause a high degree of condensation; the relative content of  $\mu_4$ - and  $\mu_3$ -oxo ligands is around twice that found for  $\{\text{Mo}_{18}\}$ -type Dawson or  $\{\text{Mo}_{12}\}$ -type Keggin anions. The significance of the encapsulation for the solid state is furthermore reflected by the very close interaction between surface oxo ligands of the anions present in **1** and **2** and the  $\text{HMTAH}^+$  cations; there are 18 short hydrogen-bonded cluster surface oxygen-to-cation interactions for the anion

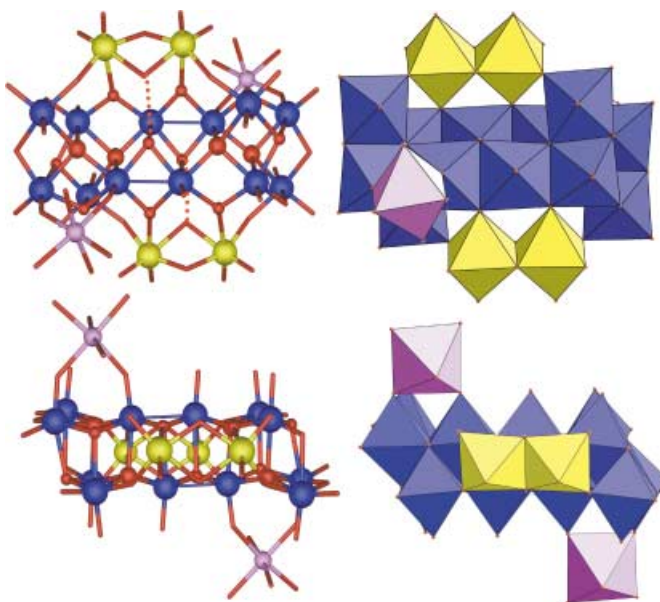


**Figure 2.** Ball-and-stick (left) and polyhedral representations (right) of the crystal structure of the  $[\text{Fe}_2(\text{H}_2\text{O})_8\text{H}_2\text{Mo}^{\text{V}}_4\text{Mo}^{\text{VI}}_{12}\text{O}_{52}]^{6-}$  anion in **2** (top views above and side views below). The main  $\{\text{Mo}_{12}\}$  body is shown in blue, the two  $\{\text{Mo}_2\}$  “wings” in yellow, and the Fe positions in purple. The oxo ligands and the hydrogen-bonded interactions are represented in the same style as Figure 1.



present in **1** and **14** for the anion in **2**. These interactions are in the range  $2.581(7) \leq d[\text{E}(\text{H})\cdots\text{O}(\text{Mo})] \leq 3.140(5) \text{ \AA}$ , where  $\text{E} = \text{N}, \text{C}$ ; there are an additional 18 longer contacts for **1** and 10 for **2** in the range  $3.157(5) \leq d[\text{E}(\text{H})\cdots\text{O}(\text{Mo})] \leq 3.296(3) \text{ \AA}$ . Furthermore, while the anion layers in **1** are effectively separated from each other by two cation layers, the separation in **2** involves only one cation layer, which permits limited cluster A-cation-cluster B contacts: In **2** the HMTAH<sup>+</sup> cations are associated via strong (N)H $\cdots$ O(Mo) hydrogen bonds to cluster A and via weak (C)H $\cdots$ O(Mo) contacts to a neighboring cluster B. This analysis shows that both of the clusters are extensively linked to the HTMAH<sup>+</sup> cations via hydrogen bonds; Figure 3 illustrates that the cluster anions are effectively covered, or “shrink-wrapped” by the HTMAH<sup>+</sup> cations in the solid state.

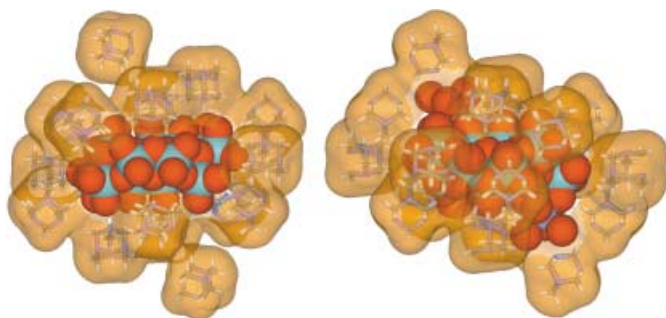


**Figure 3.** A representation of the extent of the encapsulation of the cluster anions present in compounds **1** (left) and **2** (right). The cluster anion is shown by a space-filling representation and the HMTAH<sup>+</sup> cluster cations are shown as sticks with a transparent space-filling surface over the cations.

Although cation–anion association will be present in solution, encouraged by both electrostatic and hydrogen-bonding effects, the extent of the interactions seen in the solid state also appears to play a crucial role in solution. This is because experiments attempting to synthesize the {Mo<sub>16</sub>} cluster under similar reaction conditions (e.g., pH value, concentrations, ionic strength, and temperature), but with different large cations (e.g., [HN(CH<sub>2</sub>CH<sub>2</sub>OH)<sub>3</sub>]<sup>+</sup>), result in the formation of well-known spherical-type POMo clusters of the Dawson type.<sup>[15]</sup> Furthermore, the isolation of compounds **1** and **2** is only possible in a narrow pH range (4.0–4.5) at room temperature in the presence of a large excess of HMTAH<sup>+</sup> (HMTAH<sup>+</sup>:{Mo<sub>16</sub>} = 60:1). Dissolving compounds **1** and **2** in the presence of different cations appears to result in the decomposition of the cluster anions.<sup>[10]</sup>

The importance of the encapsulation event in the “shrink-wrapping” synthesis of these clusters is also supported by the fact that there is only one other structural type comprising an {Mo<sub>16</sub>} nuclearity framework reported previously,<sup>[16]</sup> [X<sub>n</sub>Mo<sub>16</sub>(OH)<sub>12</sub>O<sub>40</sub>]<sup>(8–n)–</sup> (where X<sub>n</sub> is Na or H<sub>2</sub>) but, in contrast to the fundamentally new topology presented here, this {Mo<sub>16</sub>} framework is based upon the well-known spherical topology and adopts the high *T<sub>d</sub>* symmetry of the inner  $\epsilon$ -Keggin motif.<sup>[8]</sup> In this case the highly charged central, compact, and fully reduced {Mo<sup>V</sup><sub>12</sub>}  $\epsilon$ -Keggin unit is stabilized

by the condensation of four corner-sharing Mo<sup>VI</sup>O<sub>6</sub> units. Although the cluster types in **1** and **2** bear no geometrical resemblance to the  $\epsilon$ -Keggin-type {Mo<sub>16</sub>} ion,<sup>[17]</sup> in analogy their two {Mo<sub>2</sub>} wing fragments are also linked to their backbone fragments exclusively in a corner-sharing mode. Therefore it is interesting to note that the removal of those {Mo<sup>VI</sup><sub>2</sub>O<sub>6</sub>} wings would produce an {Mo<sub>12</sub>} cluster, yet to be isolated, with the same nuclearity of a classical Keggin ion, but with a new topology for an {Mo<sub>12</sub>} fragment (shown in blue in Figures 1 and 2).

In summary, this work demonstrates that it is possible to redefine the structures of lower-nuclearity POMos away from the symmetrical spherical structures. In further work we will attempt to incorporate other types of electrophiles, for example Eu<sup>III</sup>, in addition to studies that aim to exploit our new cluster topology in the formation of large clusters based on this interesting building block, that utilize the nonspherical nature of this new class of POMo clusters. There are certainly many other interesting structural types to be trapped and characterized using the approach outlined here, and we expect that this will provide access to a fundamentally more diverse set of POMo-based building blocks.

## Experimental Section

**1:** Hexamethylenetetraamine (2.2 g, 15.7 mmol) was dissolved in water (20 mL) at room temperature and the resulting solution was acidified with 1.2 mL hydrochloric acid (37%). To the resulting solution Na<sub>2</sub>MoO<sub>4</sub>·2H<sub>2</sub>O (0.96 g, 4.0 mmol) and Na<sub>2</sub>S<sub>2</sub>O<sub>4</sub> (0.07 g, 0.44 mmol) were added simultaneously while stirring. After addition the color of the solution changed firstly to green, then to yellowish green, and finally to brown (the pH of the solution was 4.0–4.5). The solution mixture was filtered and sealed in a small vial, from which brown crystals of **1** formed over a period of two days in a yield of 0.20 g (18%; all yields calculated based on Mo<sup>[10]</sup>). IR (KBr disk):  $\tilde{\nu} = 3443, 1631, 1461, 1400, 1378, 1308, 1289, 1253, 1203, 1018, 1009, 978, 926, 817, 794, 658 \text{ cm}^{-1}$ ; elemental analysis calcd for C<sub>60</sub>H<sub>200</sub>Mo<sub>16</sub>N<sub>40</sub>O<sub>86</sub>: C 16.40, H 4.59, N 12.75; found: C 16.28, H 4.13, N 12.77%.

**2:** The brown solution obtained in the synthesis of **1** was left undisturbed for 6 h at room temperature. After this period the solution was added to a solution of FeSO<sub>4</sub>·7H<sub>2</sub>O (0.18 g, 0.65 mmol) in water (50 mL), which had previously been acidified with 0.2 mL hydrochloric acid (37%). The mixture was stirred for two minutes and quickly filtered. Subsequently the color of the solution changed slightly from brown to reddish brown, and dark-brown crystals of **2** formed overnight. Yield: 0.25 g (28%). IR (KBr disk):  $\tilde{\nu} = 3426, 1637, 1462, 1401, 1384, 1259, 1017, 980, 925, 887, 639 \text{ cm}^{-1}$ ; elemental analysis calcd for C<sub>36</sub>H<sub>112</sub>Fe<sub>2</sub>Mo<sub>16</sub>N<sub>24</sub>O<sub>68</sub>: C 11.96, H 3.12, N 9.30; found: C 11.90, H 3.00, N 8.96%.

Received: April 9, 2003 [Z51615]

**Keywords:** cluster compounds · molybdenum · polyoxometalates · self-assembly · supramolecular chemistry

- [1] A. Müller, E. Beckmann, H. Bögge, M. Schmidtman, A. Dress, *Angew. Chem.* **2002**, *114*, 1210–1215; *Angew. Chem. Int. Ed.* **2002**, *41*, 1162–1167; L. Cronin, C. Beugholt, E. Krickemeyer, M. Schmidtman, H. Bögge, P. Kögerler, T. K. K. Luong, A. Müller, *Angew. Chem.* **2002**, *114*, 2929–2932; *Angew. Chem. Int. Ed.* **2002**, *41*, 2805–2808; A. Müller, E. Krickemeyer, H. Bögge,

- M. Schmidtman, P. Kögerler, C. Rosu, E. Beckmann, *Angew. Chem.* **2001**, *113*, 4158–4161; *Angew. Chem. Int. Ed.* **2001**, *40*, 4034–4037; A. Müller, S. Q. N. Shah, H. Bögge, M. Schmidtman, *Nature* **1999**, *397*, 48–50; A. Müller, E. Krickemeyer, H. Bögge, M. Schmidtman, F. Peters, *Angew. Chem.* **1998**, *110*, 3567–3571; *Angew. Chem. Int. Ed.* **1998**, *37*, 3360–3363; A. Müller, E. Krickemeyer, J. Meyer, H. Bögge, F. Peters, W. Plass, E. Diemann, S. Dillinger, F. Nonnenbruch, M. Randerath, C. Menke, *Angew. Chem.* **1995**, *107*, 2293–2295; *Angew. Chem. Int. Ed. Engl.* **1995**, *34*, 2122–2124.
- [2] H. D. Zeng, G. R. Newkome, C. L. Hill, *Angew. Chem.* **2000**, *112*, 1842–1844; *Angew. Chem. Int. Ed.* **2000**, *39*, 1772–1774.
- [3] T. F. Otero, S. A. Cheng, E. Coronado, E. M. Ferrero, C. J. Gomez-Garcia, *ChemPhysChem* **2002**, *3*, 808–811.
- [4] D. A. Judd, J. H. Nettles, N. Nevins, J. P. Snyder, D. C. Liotta, J. Tang, J. Ermoloeff, R. F. Schinazi, C. L. Hill, *J. Am. Chem. Soc.* **2001**, *123*, 886–897.
- [5] A. Müller, P. Kögerler, C. Kuhlmann, *Chem. Commun.* **1999**, 1347–1358.
- [6] E. Cadot, F. Sécheresse, *Chem. Commun.* **2002**, 2189–2197; R. J. Errington, R. L. Wingad, W. Clegg, M. R. J. Elsegood, *Angew. Chem.* **2000**, *112*, 4042–4044; *Angew. Chem. Int. Ed.* **2000**, *39*, 3884–3886.
- [7] P. Wang, Y. Yuan, Z. B. Han, G. Y. Zhu, *J. Mater. Chem.* **2001**, *11*, 549–553.
- [8] a) P. Mialane, A. Dolbecq, L. Lisnard, A. Mallard, J. Marrot, F. Sécheresse, *Angew. Chem.* **2002**, *114*, 2504–2507; *Angew. Chem. Int. Ed.* **2002**, *41*, 2398–2401; b) J. F. Keggin, *Nature* **1933**, *131*, 908–909; A search of the CSD database revealed that all of the pure POMo-based clusters in the Mo<sub>10</sub>–Mo<sub>18</sub> range have spherical topologies.
- [9] M. T. Pope, A. Müller, *Angew. Chem.* **1991**, *103*, 56–70; *Angew. Chem. Int. Ed. Engl.* **1991**, *30*, 34–48.
- [10] a) The work presented here is the first example of the isolation of a nonspherical “shrink-wrapped” cluster-type using bulky cations, however HMTA has been utilized in the synthesis of POM-based clusters previously. For example, see: T. Duraismy, N. Ojha, A. Ramanan, J. J. Vittal, *Chem. Mater.* **1999**, *11*, 2339–2349. b) The relatively low yield of **1** could be explained by the fact that the by-product, Na<sub>2</sub>(HTMAH<sub>2</sub>)<sub>2</sub>[Mo<sub>7</sub>O<sub>24</sub>], was found to be produced in a yield of approximately 60%, as verified by crystallographic analysis. This by-product is either produced during the formation of **1** in a competing reaction or by decomposition of **1** in the presence of the mother liquor; this decomposition appears to be accelerated upon heating.
- [11] Crystal data and structure refinements for **1** and **2**: (C<sub>6</sub>H<sub>13</sub>N<sub>4</sub>)<sub>10</sub>[H<sub>2</sub>Mo<sub>16</sub>O<sub>52</sub>]·34 H<sub>2</sub>O **1**: C<sub>60</sub>H<sub>200</sub>Mo<sub>16</sub>N<sub>40</sub>O<sub>86</sub>, *M<sub>r</sub>* = 4393.64, a platelike crystal (0.25 × 0.20 × 0.09 mm) was analyzed with a Kappa CCD diffractometer using MoK<sub>α</sub> radiation (*λ* = 0.71073 Å) at 150(2) K; triclinic, space group *P* $\bar{1}$ , *a* = 13.81780(10), *b* = 16.1705(2), *c* = 17.0835(2) Å, *α* = 95.1180(10), *β* = 112.5320(10), *γ* = 96.7450(10)°, *V* = 3463.68(6) Å<sup>3</sup>, *Z* = 1, *ρ*<sub>calcd</sub> = 2.106 g cm<sup>−3</sup>, *μ*(MoK<sub>α</sub>) = 1.513 cm<sup>−1</sup>, *F*(000) = 2200, 76303 reflections measured, of which 20204 were independent, 910 refined parameters, *R*1 = 0.0368, *wR*2 = 0.0886. For (C<sub>6</sub>H<sub>13</sub>N<sub>4</sub>)<sub>6</sub>[Fe<sub>2</sub>(H<sub>2</sub>O)<sub>8</sub>H<sub>2</sub>Mo<sub>16</sub>O<sub>52</sub>]·8 H<sub>2</sub>O **2**: C<sub>36</sub>H<sub>112</sub>Fe<sub>2</sub>Mo<sub>16</sub>N<sub>24</sub>O<sub>68</sub>, *M<sub>r</sub>* = 3616.24 g mol<sup>−1</sup>; 0.47 × 0.35 × 0.03 mm; monoclinic, space group *P*2<sub>1</sub>/*a*, *a* = 13.87320(10), *b* = 25.6770(2), *c* = 15.80270(10) Å, *β* = 108.8090(10)°, *V* = 5328.66(7) Å<sup>3</sup>, *Z* = 2, *ρ*<sub>calcd</sub> = 2.254 g cm<sup>−3</sup>, *μ*(MoK<sub>α</sub>) = 2.182 cm<sup>−1</sup>, *F*(000) = 3528, 79325 reflections measured, of which 10413 were independent, 758 refined parameters, *R*1 = 0.0371, *wR*2 = 0.1066. In both structures the distance between the two oxygen atoms (indicated by the dotted lines in Figures 1 and 2) is 2.732(5) Å, which is consistent with the presence of a medium-to-strong hydrogen-bonded interaction between the two atoms. Although these protons could not be located unambiguously from the crystallographic data (although a very small peak could be identified in the Fourier difference map), the two μ<sub>3</sub>-oxo ligands bridging the Mo<sup>V</sup> atoms are the only positions that could support a proton. CCDC-205853 (**1**) and CCDC-205854 (**2**) contain the supplementary crystallographic data for this paper. These data can be obtained free of charge via [www.ccdc.cam.ac.uk/conts/retrieving.html](http://www.ccdc.cam.ac.uk/conts/retrieving.html) (or from the Cambridge Crystallographic Data Centre, 12, Union Road, Cambridge CB21EZ, UK; fax: (+44)1223-336-033; or deposit@ccdc.cam.ac.uk).
- [12] I. D. Brown in *Structure and Bonding in Crystals, Vol. II* (Eds.: M. O'Keeffe, A. Navrotsky), Academic Press, New York, **1981**, pp. 1–30; N. E. Breese, M. O'Keeffe, *Acta Crystallogr. Sect. B* **1991**, *47*, 192–197; The UV/Vis spectrum for complex **1** shows a broad absorption band with *λ*<sub>max</sub> ≈ 311 nm (sh).
- [13] H. K. Chae, W. G. Klempner, T. A. Marquart, *Coord. Chem. Rev.* **1993**, *128*, 209–224.
- [14] The partial charges on O(Mo3) and O(Mo4) were deduced by extended Hückel–MO and preliminary DFT studies and further computational and synthetic work, which examines the nature of the addition of electrophiles to O(Mo3) and O(Mo4), is ongoing and the results will be reported in due course.
- [15] Replacement of HMTAH<sup>+</sup> by, for instance, [HN(CH<sub>2</sub>CH<sub>2</sub>OH)<sub>3</sub>]<sup>+</sup>, results in a Dawson-type POMo cluster containing heteroatoms which appear to originate from the reducing agent. (D.-L. Long, P. Kögerler, L. J. Farrugia, L. Cronin, unpublished results).
- [16] M. I. Khan, A. Müller, S. Dillinger, H. Bögge, Q. Chen, J. Zubietta, *Angew. Chem.* **1993**, *105*, 1811–1813; *Angew. Chem. Int. Ed. Engl.* **1993**, *32*, 1780–1782; M. I. Khan, Q. Chen, J. Salta, C. J. O'Connor, J. Zubietta, *Inorg. Chem.* **1996**, *35*, 1880–1901.
- [17] A. Müller, J. Meyer, E. Krickemeyer, C. Beugholt, H. Bögge, F. Peters, M. Schmidtman, P. Kögerler, M. J. Koop, *Chem. Eur. J.* **1998**, *4*, 1000–1006.